MONTHLY WEATHER REVIEW

VOLUME 94, NUMBER 11

NOVEMBER 1966

LARGE-SCALE BALANCE OF KINETIC ENERGY IN THE ATMOSPHERE

ERNEST C. KUNG

Geophysical Fluid Dynamics Laboratory, Environmental Science Services Administration, Washington, D.C.

ABSTRACT

The vertical distribution and seasonal variation of the kinetic energy balance of the atmosphere are studied. From 11 months' daily wind and geopotential data during 1962 and 1963 over North America, the generation due to the work done by the horizontal pressure force, the local change, the horizontal outflow, and the vertical transport are evaluated for 20 pressure layers from the surface to 50 mb. The dissipation is then obtained as the residual to balance the kinetic energy equation.

The generation and dissipation are at a maximum in the planetary boundary layer. They decrease gradually to a minimum in the mid-troposphere, increase again to the second maximum in the upper part of the atmosphere, then decrease again farther upward. The generation and dissipation are approximately balanced in the lower troposphere, particularly in the boundary layer, for the large-scale domain of analysis.

The generation and dissipation of the kinetic energy are significantly large both in the lower troposphere and in the upper part of the atmosphere. However, in view of the amount of the kinetic energy contained in different portions of the atmosphere, the energy generation and dissipation are most intense in the lower troposphere, especially in the boundary layer. The efficiency of the dissipation in different portions of the atmosphere is also examined in terms of the depletion time. The depletion time is orders of magnitude shorter in the boundary layer than in the mid-troposphere.

A seasonal change of the energetics is depicted for the one-year period by means of the pressure-time cross sections.

CONTENTS

1. INTRODUCTION

While other major processes in the fundamental atmospheric energy cycle have been and are being studied in great detail, the problem of the kinetic energy dissipation is rather untouched. In a previous paper (Kung [5]), as a preliminary of a systematic approach to the energy dissipation problem, the kinetic energy budget and dissipation were studied in their various partitionings with six months' daily wind and geopotential data during 1962 and 1963 over North America. Of special interest in the previous paper was the devising of a technique to evaluate the cross-isobar flow, which enabled the direct computation of the kinetic energy generation with observed wind and geopotential data at individual isobaric surfaces. This suggests the feasibility of further investigations of the kinetic energy budget in detail, which might provide a broader basis to approach the problem of energy dissipation.

In the present study, attention is focused on the vertical structure and seasonal variation of the balance of the kinetic energy. Various kinetic energy parameters, including the generation, local change, horizontal outflow,

and vertical transport were evaluated for 20 pressure layers from the surface to 50 mb., using 11 months' daily wind and geopotential data during 1962 and 1963 over North America. To provide a broader observational basis to attack the problem of energy dissipation, we have to *evaluate the dissipation without employing specific theories in this connection.* Thus, we obtained the dissipation as the residual to balance other energy parameters in the kinetic energy equation. The seasonal and annual means of evaluated parameters are presented and examined in their vertical resolution and in total, and the time series of monthly means of these parameters are depicted as a progress of seasons.

Since the uniform and dense aerological network in existence over North America during recent years provides a convenient area for this analysis, and since useful results may be expected with data from a network of this size, the data coverage is still restricted to the continent at this stage of the study. However, it is hoped that this constraint will be eased gradually as the study proceeds in the future.

2. SCHEME OF ANALYSIS AND DATA

In the discussions to follow, $\mathbf{V}$ is the vector of the horizontal wind, u the eastward wind component, v the northward wind component, t the time, g the acceleration of gravity, ϕ the geopotential, f the Coriolis parameter, $-\mathbf{F}$ the vector of the frictional force per unit mass, p the pressure, s the boundary of the continental region, $\mathbf{n}$ the outward-directed unit vector normal to the continental boundary, $\mathbf{k}$ the unit vector in the vertical direction, A the area of the continental region on the earth, and ∇ the horizontal del operator along an isobaric surface. Also, the vertical p-velocity ω and kinetic energy k are:

$$\omega=\frac{dp}{dt} \tag{1}$$

and

$$k=\tfrac{1}{2}\mathbf{V}\cdot\mathbf{V}=\tfrac{1}{2}(u^2+v^2) \tag{2}$$

The domain mean of a dummy variable $\overline{q}$ is defined by

$$\overline{q}=\frac{1}{A}\int_A q\,dA \tag{3}$$

and the horizontal bar notation will be used to indicate the area mean of a quantity over the continent throughout this paper. Using the equation of motion as

$$\frac{d\mathbf{V}}{dt}=-\nabla\phi-\mathbf{k}\times f\mathbf{V}-\mathbf{F}$$

or

$$\frac{\partial\mathbf{V}}{\partial t}+(\mathbf{V}\cdot\nabla)\mathbf{V}+\omega\frac{\partial\mathbf{V}}{\partial p}=-\nabla\phi-\mathbf{k}\times f\mathbf{V}-\mathbf{F} \tag{4}$$

and the continuity equation as

$$\nabla\cdot\mathbf{V}+\frac{\partial\omega}{\partial p}=0 \tag{5}$$

we obtain the kinetic energy equation as the scalar product of the equation of motion and the horizontal wind vector $\mathbf{V}$, and then solve for the kinetic energy dissipation E

$$-E=-\mathbf{V}\cdot\mathbf{F}=\frac{\partial k}{\partial t}+\nabla\cdot\mathbf{V}k+\frac{\partial\omega k}{\partial p}+\mathbf{V}\cdot\nabla\phi \tag{6}$$

Integrating equation (6) over the continental area, we then have the area mean kinetic energy equation over the continent

$$-\overline{E}=-\overline{\mathbf{V}\cdot\mathbf{F}}=\frac{\partial\overline{k}}{\partial t}+\frac{1}{A}\oint_c \mathbf{V}k\cdot\mathbf{n}\,ds+\frac{\partial\overline{\omega k}}{\partial p}+\overline{\mathbf{V}\cdot\nabla\phi} \tag{7}$$

The processes related to the energy dissipation $\overline{E}$ in equation (7) will be termed as follows throughout the discussion:

$-\overline{\mathbf{V}\cdot\nabla\phi}$=generation or generation due to the work done by the horizontal pressure force

$\frac{\partial\overline{k}}{\partial t}$=local change

$\frac{1}{A}\oint_c \mathbf{V}k\cdot\mathbf{n}\,ds$=horizontal outflow

$\frac{\partial\overline{\omega k}}{\partial p}$=vertical transport

The vertical p-velocity ω is obtained by making use of the continuity equation (5) as

$$\omega_{p_1}=\int_{p_1}^{p_2}\nabla\cdot\mathbf{V}\,dp+\omega_{p_2} \tag{8}$$

where ω_{p_1} and ω_{p_2} are ω at pressure levels p_1 and p_2. Thus, for the area mean we have

$$\overline{\omega_{p_1}}=\frac{1}{A}\int_{p_1}^{p_2}\oint_c \mathbf{V}\cdot\mathbf{n}\,ds\,dp+\overline{\omega_{p_2}} \tag{9}$$

In computing $\overline{\omega}$ by equation (9), it is assumed that $\overline{\omega}=0$ at the surface level.

Since the hazard caused by errors in estimating the wind divergence is expected to decrease in proportion to the characteristic length-scale of the domain of analysis, and since for our domain of analysis it may be expected that $\overline{\omega}\,\overline{k}$ contributes significantly to $\overline{\omega k}$, $\overline{\omega}\,\overline{k}$ is substituted for $\overline{\omega k}$ in evaluation of the vertical transport. (Sec. 4)

In order to use the actual observed wind data at individual stations to estimate $-\mathbf{V}\cdot\nabla\phi$, the horizontal gradient of the geopotential $\nabla\phi$ is computed by the technique described in the previous paper (see Kung [5]) with a modification that the reciprocal of the square of the distance between observational stations is used as the weighting factor in the least square selections process of $\partial\phi/\partial x$ and $\partial\phi/\partial y$.

The quantity per unit mass is vertically integrated for the mass of a pressure layer per unit area, making use of the hydrostatic equation. This will be clearly indicated by the physical units in use. However, for the sake of

simplicity in presentation, the notation of vertical integral will be omitted. Thus, presentation of an area mean of a dummy energy parameter $\overline{X}$ in some units per unit area will be understood to mean

$$\frac{1}{g}\int_{p_1}^{p_2}\overline{X}dp$$

for a specified pressure layer between p_1 and p_2 where $p_2>p_1$.

The daily aerological (wind and geopotential) data by rawinsonde/radiosonde observations at 00 GMT over the North American Continent and some surrounding regions from February 1962 through January 1963 were obtained from the MIT General Circulation Data Library for the Northern Hemisphere (the National Science Foundation Grant GP 820 and GP 3657). September 1962 data were not utilized, because of a technical difficulty in editing the input data tape in our possession; thus 11 months' data were available for analysis.

The distributions of the aerological stations and the continental boundary in the analysis are shown in figure 1. A total of 101 stations are on or within the continental boundary, and an additional 18 stations outside the boundary were also used to assist in the evaluation of $\nabla\phi$ and in data editing. The computation was carried out on a daily basis for each of the 20 pressure layers from the surface to the 50-mb. level utilizing the data at 21 specific isobaric levels, i.e., surface, 950 mb. to 100 mb. at 50-mb. intervals, 70 mb., and 50 mb. The $\nabla\phi$ at the surface level was computed with the geopotential height of the 1,000-mb. level. The daily aerological data of each station were examined carefully, and the stations without a wind report or with suspicious data were omitted in the computation at each particular pressure level. The days with comparatively few available stations were eliminated from the analysis; the first day's data of each month were used only to compute $\partial\overline{k}/\partial t$ for the next day. A monthly value of a physical quantity was obtained by averaging the values of individual available days in the month; a seasonal mean value was obtained by averaging the monthly values, and then an annual mean value was obtained by averaging the seasonal mean values. Table 1 shows days available for monthly averages and average numbers of daily available stations for each month at five characteristic levels.

The variations of computed energy parameters in the time series are large and interesting. Though a rather thorough statistical treatment of the variance of the computed parameters is planned in the future with a much larger data sample (see Kung, Bryson, Lenschow [6] for a simple example of analysis of variance), at this stage of the study we depict only the obviously largest source of variation, the quasi-cyclic nature of the atmospheric process, in terms of monthly and seasonal variations. As for the variation of the daily computed

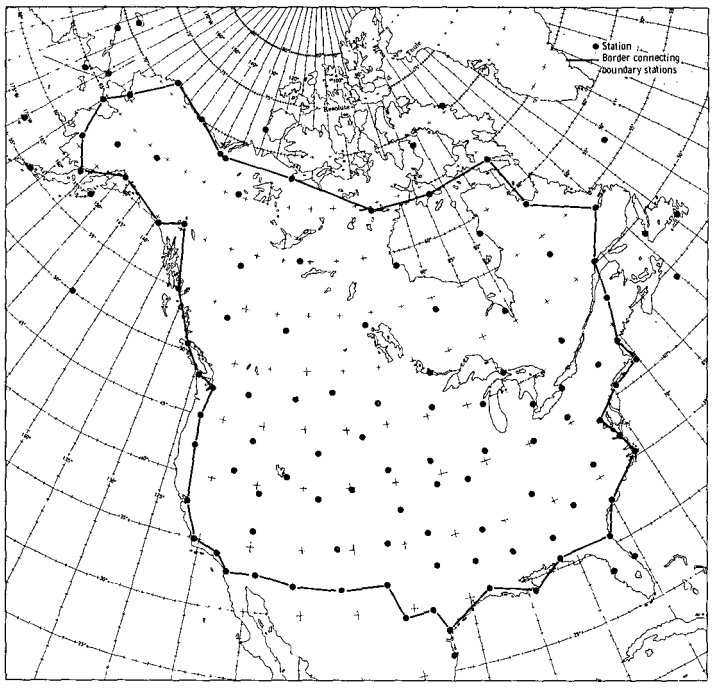

FIGURE 1.—Aerological stations and continental boundary.

parameters, only the pressure-time cross sections of the generation and horizontal outflow during June 1962 are shown separately in figures 2 and 3 as examples. For this reference may be made to the earlier paper (Kung [5]).

3. VERTICAL DISTRIBUTION OF KINETIC ENERGY BALANCE

To study the vertical structure of the kinetic energy balance with equation (7), the estimate of the generation $-\mathbf{V}\cdot\nabla\phi$ is vital. The term may be expressed:

$$-\overline{\mathbf{V}\cdot\nabla\phi}=-\overline{\nabla\cdot\mathbf{V}\phi}-\frac{\partial\overline{\omega\phi}}{\partial p}-\overline{\omega\alpha} \qquad (10)$$

TABLE 1.—*Available days for monthly averages and averaged number of daily available stations for each month at characteristic pressure levels*

Month	Avail. days of month	Total avail. days	Monthly average number of daily available stations											
			Surface		700 mb.		500 mb.		300 mb.		100 mb.		50 mb.	
			(1)	(2)	(1)	(2)	(1)	(2)	(1)	(2)	(1)	(2)	(1)	(2)
Jan. 1963	2–31	30	86	38	83	37	79	36	71	33	56	27	48	23
Feb. 1962	3–27	25	86	38	85	38	83	37	76	34	64	29	60	28
Mar. 1962	2–30	29	86	40	85	39	85	39	79	36	69	30	65	29
Apr. 1962	2–17, 24–30	23	87	39	86	38	84	38	79	36	70	32	68	31
May 1962	2–30	29	88	39	86	38	86	38	82	36	76	34	73	32
Jun. 1962	2–30	29	87	39	86	38	85	38	82	36	77	34	74	33
Jul. 1962	2–20	19	83	37	81	36	81	36	79	35	74	33	72	32
Aug. 1962	2–25	24	87	39	85	38	85	38	82	37	77	35	74	33
Oct. 1962	2–31	30	86	38	84	37	83	36	77	34	70	32	66	30
Nov. 1962	2–24	23	87	39	84	38	83	37	77	35	69	31	65	30
Dec. 1962	2–30	29	86	39	84	38	81	37	74	35	64	30	57	27

(1) Total available stations on and within continental boundary.
(2) Continental stations on the boundary.

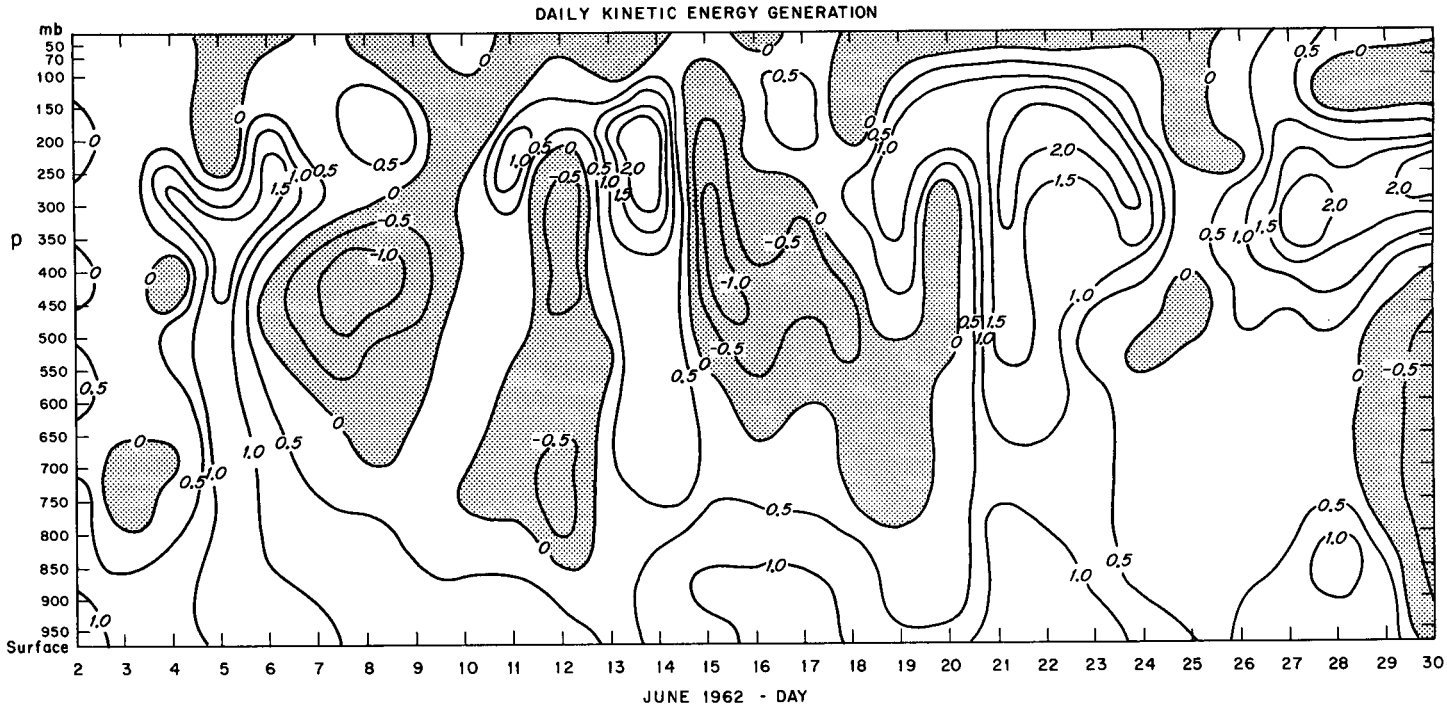

FIGURE 2.—Pressure-time cross section of daily kinetic energy generation $-\overline{\mathbf{V}\cdot\nabla\phi}$ in units of (watts/m.²)/50 mb. in June 1962. Destruction of kinetic energy is stippled.

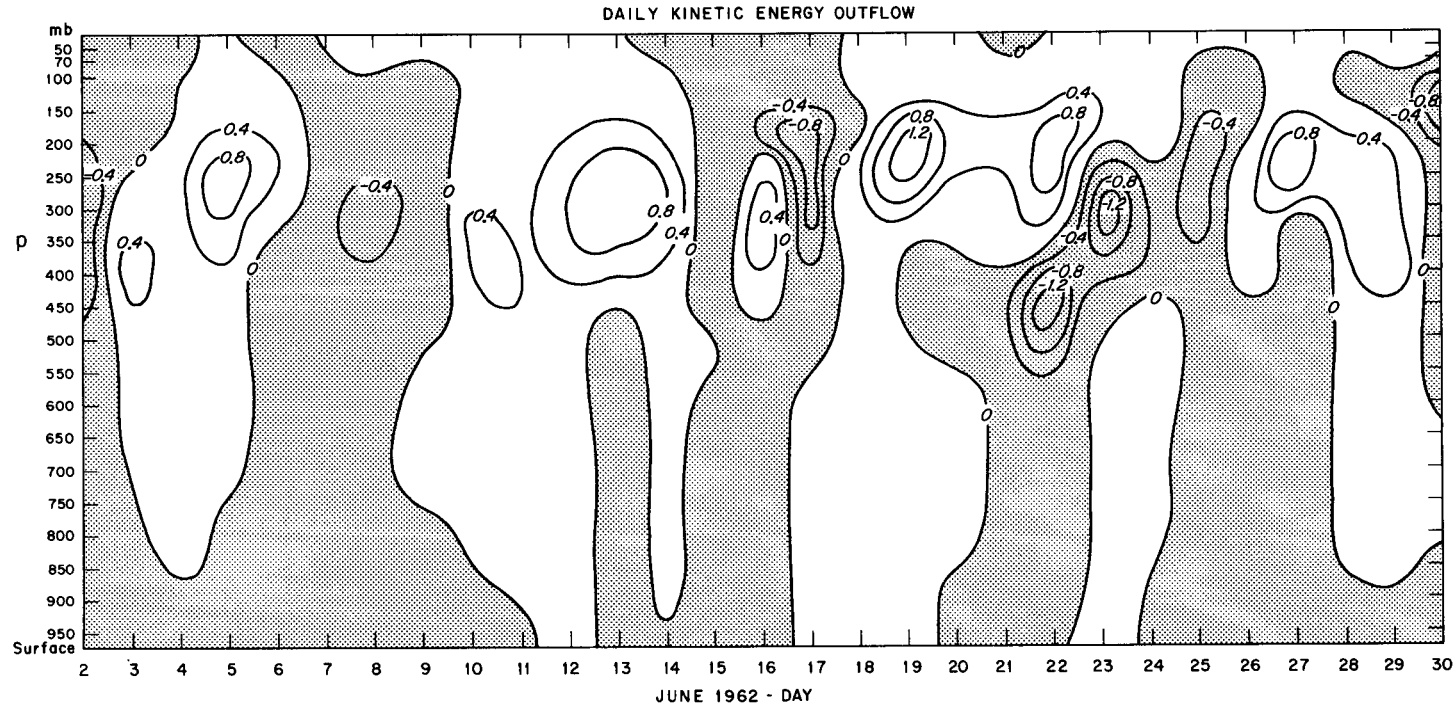

FIGURE 3.—Pressure-time cross section of daily kinetic energy horizontal outflow $\frac{1}{A}\oint_c \mathbf{V}k\cdot n ds$ in units of (watts/m.²)/50 mb. in June 1962. Inflow of kinetic energy is stippled.

where α is the specific volume of air. While the conversion term $-\overline{\omega\alpha}$ may be regarded as the release of available potential energy, $-\overline{\nabla\cdot\nabla\phi}$ and $-(\partial\overline{\omega\phi}/\partial p)$ may be regarded as the redistribution terms to appear as the actual generation of the kinetic energy. For the study of the kinetic energy generation of hemispherical or global scale, the conversion term $-\overline{\omega\alpha}$ is customarily evaluated instead of $-\mathbf{V}\cdot\nabla\phi$, since if equation (10) is integrated over the entire mass of the atmosphere, M, we have

$$-\int_M \overline{\mathbf{V}\cdot\nabla\phi}dM=-\int_M \overline{\omega\alpha}dM \qquad (11)$$

However, to obtain the dissipation $\overline{E}$ as the residual of equation (7) in individual atmospheric layers using the network data over a continent, $-\overline{\nabla\cdot\mathbf{V}\phi}$ and $-\partial\overline{\omega\phi}/\partial p$ must also be evaluated as well as $-\omega\alpha$, especially because the vertical profile of $-\overline{\omega\alpha}$ is expected to be very different from that of $-\mathbf{V}\cdot\nabla\phi$ (see Smagorinsky, Manabe, and Holloway [15]).

Moreover, a direct estimate of $-\overline{\mathbf{V}\cdot\nabla\phi}$ with observed wind and geopotential data is highly desirable, since most of the observational studies of $-\overline{\omega\alpha}$, which depends mainly on the spatial correlation of ω and α, depend on the estimation of ω from operationally smoothed and modified data on the basis of the adiabatic, quasi-geostrophic models. It also should be noticed that the evaluation of $-\overline{\mathbf{V}\cdot\nabla\phi}$ essentially depends on the ageostrophic component of the observed wind.

Seasonal and annual means of the kinetic energy balance for the 20 pressure layers from the surface to the 50-mb. level are presented in tables 2 through 6; table 2 shows averages of January 1963, and February and December 1962 values as the winter means; table 3 shows averages of March, April, and May 1962 values as the spring means; table 4 shows averages of June, July, and August 1962 values as the summer means; table 5 shows averages of September, October, and November 1962 values as the fall means; and table 6 shows averages of the four seasonal values as the annual mean values. The missing September 1962 values (see section 2) were linearly interpolated between August and October 1962 values, since plotting of the mean monthly energy processes in pressure-time cross sections (see section 6 and figs. 8 through 10) seems to allow us to fill in this particular gap of the time series in this way. For easier inspection, the vertical structure of the kinetic energy balance is plotted for winter in figure 4, for summer in figure 5, and for the annual in figure 6, in terms of

$$-\overline{\mathbf{V}\cdot\nabla\phi},\ -\partial\overline{k}/\partial t,\ -\frac{1}{A}\oint_c \overline{\mathbf{V}k}\cdot\mathbf{n}ds,\ -(\partial\overline{\omega k}/\partial p),\ \text{and}\ -\overline{E}.$$

By equation (7), the balance of the kinetic energy requires that

$$\overline{E}=-\overline{\mathbf{V}\cdot\nabla\phi}-\frac{\partial\overline{k}}{\partial t}-\frac{1}{A}\oint_c \overline{\mathbf{V}k}\cdot\mathbf{n}ds-\frac{\partial\overline{\omega k}}{\partial p}$$

TABLE 2.—*Winter mean kinetic energy budget within each pressure layer (February and December 1962, and January 1963). $\overline{k}$ is in units of 10^5 joules/m². Other quantities are in watts/m².*

Pressure layer (mb.)	$\overline{k}$	$\frac{\partial\overline{k}}{\partial t}$	$\frac{1}{A}\oint_c \overline{\mathbf{V}k}\cdot\mathbf{n}ds$	$\frac{\partial\overline{\omega k}}{\partial p}$	$-\overline{\mathbf{V}\cdot\nabla\phi}$	$\overline{E}$
*971-950	0.058	0.001	0.005	−0.004	0.742	0.740
950-900	.236	.004	.003	−.010	1.676	1.679
900-850	.297	.003	−.012	−.008	1.070	1.087
850-800	.353	.003	−.021	−.008	.605	.631
800-750	.428	.004	−.006	−.011	.447	.460
750-700	.537	.007	.032	−.022	.361	.344
700-650	.673	.012	.072	−.031	.265	.212
650-600	.842	.019	.144	−.044	.167	.048
600-550	1.049	.027	.199	−.058	.085	−.083
550-500	1.296	.036	.257	−.055	.098	−.140
500-450	1.582	.046	.390	−.091	.175	−.170
450-400	1.921	.063	.538	−.156	.425	−.020
400-350	2.297	.077	.764	−.203	.800	.162
350-300	2.696	.089	.958	−.299	1.060	.312
300-250	3.015	.100	1.179	−.425	1.161	.307
250-200	2.992	.085	1.202	−.157	1.234	.104
200-150	2.583	.065	.972	.069	1.499	.393
150-100	2.009	.061	.564	.251	1.771	.895
100-70	.937	.035	.166	.123	1.075	.751
70-50	.563	.021	.177	−.080	.689	.571

*Area mean surface pressure.

TABLE 3.—*Spring mean kinetic energy budget within each pressure layer (March, April, and May 1962). $\overline{k}$ is in units of 10^5 joules/m². Other quantities in watts/m².*

Pressure layer (mb.)	$\overline{k}$	$\frac{\partial\overline{k}}{\partial t}$	$\frac{1}{A}\oint_c \overline{\mathbf{V}k}\cdot\mathbf{n}ds$	$\frac{\partial\overline{\omega k}}{\partial p}$	$-\overline{\mathbf{V}\cdot\nabla\phi}$	$\overline{E}$
*969-950	0.048	−0.000	−0.003	0.003	0.477	0.477
950-900	.184	−.000	−.008	.008	1.276	1.276
900-850	.218	.001	−.005	.007	1.035	1.032
850-800	.250	.000	.000	.008	.746	.738
800 750	.292	.001	.010	.010	.525	.504
750-700	.346	−.002	.012	.008	.425	.407
700-650	.416	−.006	.029	.006	.336	.307
650-600	.514	−.009	.056	.004	.267	.216
600-550	.641	−.011	.054	.005	.230	.182
550-500	.798	−.015	.042	.005	.132	.100
500-450	.989	−.020	.016	.032	.026	−.002
450-400	1.237	−.020	−.055	.040	.011	.046
400-350	1.524	−.025	−.109	.048	.187	.273
350-300	1.814	−.030	−.018	.082	.376	.342
300-250	2.024	−.027	.281	.027	.446	.165
250-200	1.950	−.013	.450	−.088	.366	.017
200-150	1.530	−.013	.346	−.060	.271	−.002
150-100	.975	−.024	.182	−.011	.330	.183
100-70	.342	−.012	.033	−.042	.293	.314
70-50	.165	−.009	.015	.007	.255	.242

*Area mean surface pressure.

TABLE 4.—*Summer mean kinetic energy budget within each pressure layer (June, July, and August 1962). $\overline{k}$ is in units of 10^5 joules/m². Other quantities in watts/m².*

Pressure layer (mb.)	$\overline{k}$	$\frac{\partial\overline{k}}{\partial t}$	$\frac{1}{A}\oint_c \overline{\mathbf{V}k}\cdot\mathbf{n}ds$	$\frac{\partial\overline{\omega k}}{\partial p}$	$-\overline{\mathbf{V}\cdot\nabla\phi}$	$\overline{E}$
*968-950	0.034	0.001	−0.006	0.005	0.281	0.281
950-900	.130	.001	−.014	.012	.781	.782
900-850	.148	.001	−.010	.008	.710	.711
850-800	.166	.002	.002	.003	.508	.501
800-750	.186	.002	.009	.002	.303	.290
750-700	.211	.001	.008	.003	.171	.159
700-650	.247	.000	.007	.006	.126	.113
650-600	.293	−.001	.009	.006	.121	.107
600-550	.351	−.002	.012	.006	.101	.085
550-500	.425	−.003	.006	.005	.080	.072
500-450	.513	−.003	−.002	.005	.076	.076
450-400	.635	−.004	−.000	.006	.117	.115
400-350	.801	−.003	−.003	.001	.304	.309
350-300	1.001	−.003	.054	−.001	.651	.601
300-250	1.204	−.009	.116	−.004	.858	.755
250-200	1.233	−.011	.200	.013	.798	.596
200-150	.930	−.007	.165	−.020	.671	.533
150-100	.451	−.004	.031	−.035	.353	.361
100-70	.084	−.001	.005	−.018	.060	.074
70-50	.032	.001	.002	−.003	.014	.014

*Area mean surface pressure.

TABLE 5.—*Fall mean kinetic energy budget within each pressure layer (September, October and November 1962). $\overline{k}$ is in units of 10^5 joules/m². Other quantities in watts/m².*

Pressure layer (mb.)	$\overline{k}$	$\frac{\partial \overline{k}}{\partial t}$	$\frac{1}{A}\oint_c \mathbf{V}k\cdot\mathbf{n}ds$	$\frac{\partial \overline{\omega k}}{\partial p}$	$-\overline{\mathbf{V}\cdot\nabla\phi}$	$\overline{E}$
*967-950	0.040	0.001	0.001	−0.001	0.431	0.430
950-900	.182	.004	.005	−.006	1.268	1.265
900-850	.219	.004	−.003	−.008	.990	.997
850-800	.253	.004	−.018	−.004	.649	.667
800-750	.289	.005	−.028	−.009	.358	.390
750-700	.339	.006	−.029	−.007	.175	.205
700-650	.409	.006	−.027	−.008	.080	.109
650-600	.504	.007	−.039	−.004	.039	.075
600-550	.616	.009	−.057	−.007	−.031	.024
550-500	.753	.010	−.075	−.006	.022	.093
500-450	.927	.012	−.094	−.004	.173	.259
450-400	1.138	.020	−.113	.004	.211	.300
400-350	1.406	.029	−.161	.008	.258	.382
350-300	1.716	.031	−.137	.054	.479	.531
300-250	1.930	.028	.225	.053	.565	.259
250-200	1.901	.026	.475	−.091	.405	−.005
200-150	1.533	.024	.312	.004	.542	.202
150-100	.929	.020	.160	−.020	.585	.425
100-70	.278	.008	.052	.001	.213	.152
70-50	.112	.004	.015	−.003	.119	.103

*Area mean surface pressure.

TABLE 6.—*Annual mean kinetic energy budget within each pressure layer (February 1962 through January 1963.) $\overline{k}$ is in units of 10^5 joules/m². Other quantities are in watts/m².*

Pressure layer (mb.)	$\overline{k}$	$\frac{\partial \overline{k}}{\partial t}$	$\frac{1}{A}\oint_c \mathbf{V}k\cdot\mathbf{n}ds$	$\frac{\partial \overline{\omega k}}{\partial p}$	$-\overline{\mathbf{V}\cdot\nabla\phi}$	$\overline{E}$
*969-950	0.045	0.001	−0.001	0.001	0.483	0.482
950-900	.183	.003	−.004	.001	1.250	1.250
900-850	.220	.001	−.008	−.000	.951	.958
850-800	.256	.002	−.009	−.000	.627	.634
800-750	.298	.003	−.004	−.002	.408	.411
750-700	.359	.003	.006	−.004	.283	.278
700-650	.436	.003	.020	−.007	.202	.186
650-600	.538	.004	.043	−.009	.149	.111
600-550	.664	.006	.052	−.013	.096	.051
550-500	.818	.007	.058	−.013	.083	.031
500-450	1.003	.009	.078	−.014	.112	.039
450-400	1.233	.015	.093	−.027	.191	.110
400-350	1.507	.019	.123	−.037	.387	.282
350-300	1.807	.022	.214	−.041	.642	.447
300-250	2.043	.023	.450	−.087	.758	.372
250-200	2.019	.022	.582	−.081	.701	.178
200-150	1.644	.017	.449	−.002	.746	.282
150-100	1.091	.013	.234	.046	.760	.467
100-70	.410	.008	.064	.016	.410	.322
70-50	.218	.004	.052	−.020	.269	.233

*Area mean surface pressure.

or

Dissipation = Generation − (Local change + Horizontal outflow + Vertical transport)

As we observe immediately from the above mentioned tables and figures, the generation $-\overline{\mathbf{V}\cdot\nabla\phi}$ is the most dominant term among the directly computed parameters in determining vertical profiles of the kinetic energy balance. The second most important term is the horizontal outflow $\frac{1}{A}\oint_c \mathbf{V}k\cdot\mathbf{n}ds$, which has a significantly large value in the upper half of the atmosphere, especially around the level of the core of the jet stream (also see fig. 11). The vertical transport term $\partial\overline{\omega k}/\partial p$ acts as a modification, especially in winter, to another transport term, the horizontal outflow, but as a whole, its numerical value is rather insignificant. The local change is the least significant value. One thing may be pointed out about the insignificance of the listed $\partial\overline{k}/\partial t$ values. The total available days of data

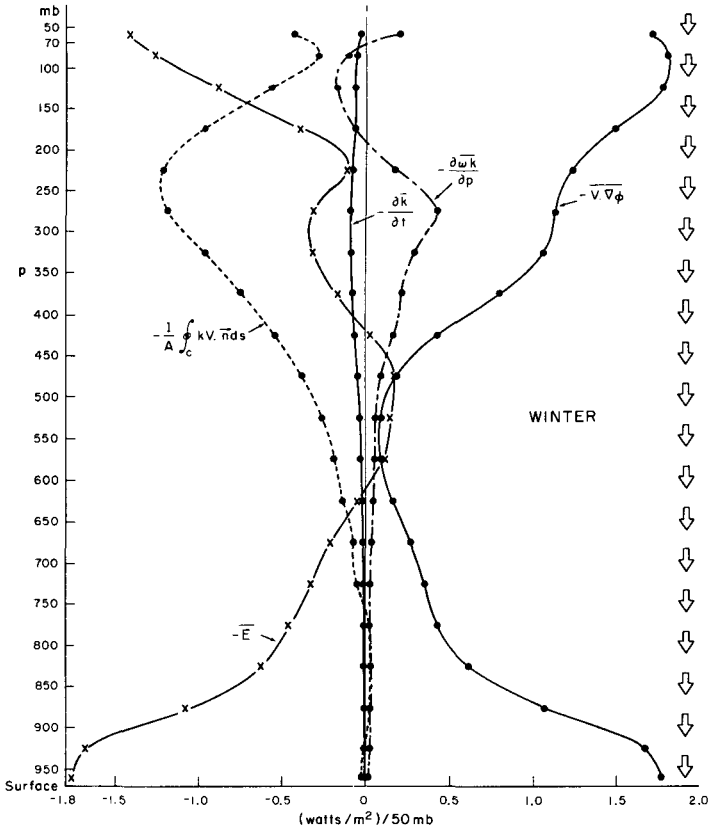

FIGURE 4.—Winter vertical profile of the kinetic energy balance (January 1963, and February and December 1962). Arrows indicate the direction of $\overline{\omega k}$.

for each month as listed in table 1 are expected to give fairly representative monthly mean values for all energy parameters after averaging of the daily values, except for $\partial\overline{k}/\partial t$. If a time average of this term (i.e., time integral of $\partial\overline{k}/\partial t$) is taken, it actually depends only on the data of the first and last days of the time series. Thus, if a time series without gaps of unavailable days is taken, $\partial\overline{k}/\partial t$ should become even smaller than the listed values. The residual term which balances the kinetic energy equation with other computed terms is taken as the dissipation $\overline{E}$ to ideally represent the energy sink.

In the previous paper (Kung [5]), and also in the nine-level model numerical experiment of the general circulation of Smagorinsky, Manabe, and Holloway [15], it was shown that strong generation takes place in the upper and lower parts of the atmosphere, while the generation in the mid-troposphere is very weak. The vertical profiles of $-\overline{\mathbf{V}\cdot\nabla\phi}$ obtained in this study essentially confirm this pattern and show additional details. Starting from the surface, we see a maximum of the generation in the planetary boundary layer, which gradually decreases toward a minimum in the mid-troposphere, and then increases again toward a second maximum in the upper part of the atmosphere. In winter, the generation in the upper part of the atmosphere extends to a very high level. This is apparently related to the upward extension and intensification of the strong circulation

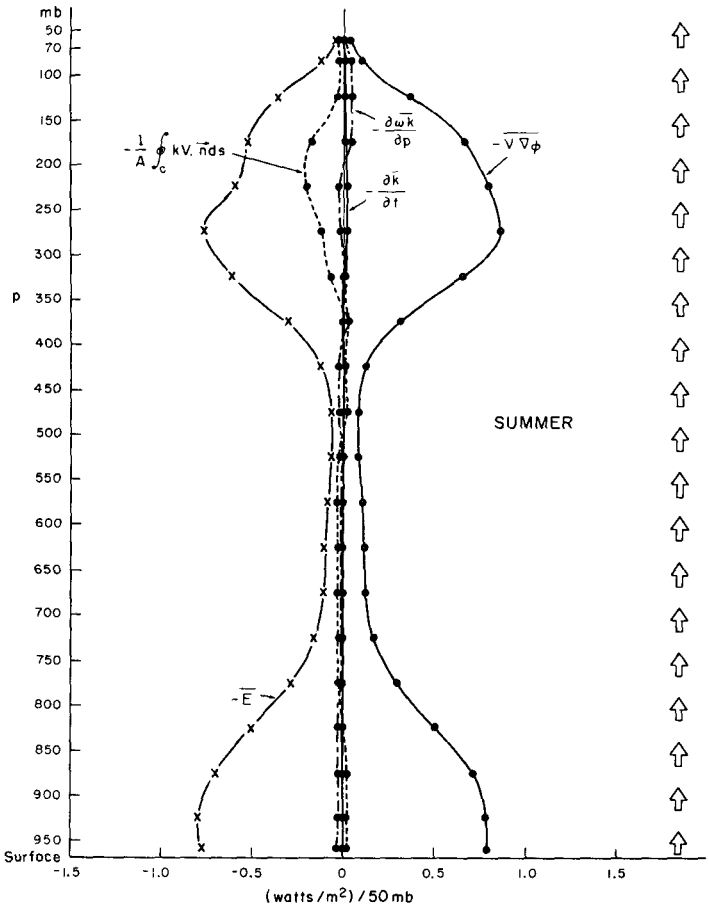

FIGURE 5.—Summer vertical profile of the kinetic energy balance (June, July, and August 1962). Arrows indicate the direction of $\overline{\omega k}$.

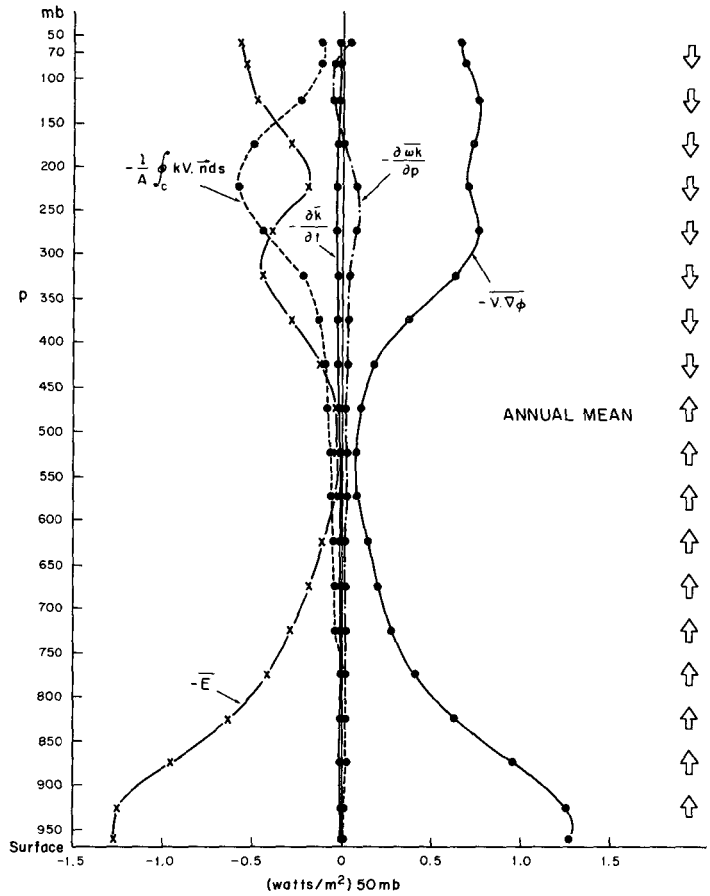

FIGURE 6.—Annual vertical profile of the kinetic energy balance (February 1962 through January 1963). Arrows indicate the direction of $\overline{\omega k}$.

pattern (see section 6 and fig. 11). The shape of the $-\overline{\mathbf{V}\cdot\nabla\phi}$ profile in figure 4, the pressure-time cross sections of the monthly values in figure 8, and also some unlisted computational results above 50 mb. with less dense station data suggest a sharp decrease of $-\overline{\mathbf{V}\cdot\nabla\phi}$ at levels above its second maximum. In summer when the upper-level circulation is weaker than in winter and decreases rapidly into the stratosphere, the $-\overline{\mathbf{V}\cdot\nabla\phi}$ sharply decreases to a second minimum of negligible value. Thus, it may be stated in general that we expect that the generation decreases again upward into the stratosphere after reaching its second maximum.

It should be noted that in the numerical experiments by Smagorinsky, Manabe, and Holloway [15], $-\overline{\omega\alpha}$ is at a maximum in the mid-troposphere while $-\overline{\mathbf{V}\cdot\nabla\phi}$ shows two maxima in the lower and upper parts of the atmosphere through $-(\partial\omega\phi/\partial p)$. In connection with the ageostrophic nature of $-\overline{\mathbf{V}\cdot\nabla\phi}$, it is noteworthy that the zonal wind component u is supergeostrophic in the middle latitudes and the meridional wind component v is subgeostrophic in the Tropics in Smagorinsky's [14] primitive equation two-level general circulation model.

In the boundary layer, we see a maximum of the dissipation $\overline{E}$ and of the generation $-\overline{\mathbf{V}\cdot\nabla\phi}$ while other energy parameters are negligibly small. This balance is maintained throughout the lower troposphere.

In the mid-troposphere where the generation is very small, the generation and the horizontal outflow are of the proper order of magnitude to determine the small dissipation as the residual, especially in winter. The dissipation in this part of the atmosphere reaches a minimum in accordance with smallness of other energy parameters. Proceeding upward from mid-troposphere, the horizontal transport and the vertical transport begin to increase in magnitude.

Both the generation and dissipation reach the second maximum in the upper part of the atmosphere. However, the horizontal outflow and vertical transport are both at their maxima, leading to important differences in the generation and dissipation profiles. The amount of the horizontal outflow is particularly significant. It is especially large at the level of the jet core when the zonal circulation is intensified, i.e., in winter, while it is rather small in summer. We may notice that in the mid-troposphere, there are several small negative $\overline{E}$ values that are given as dissipation. This result may be due to

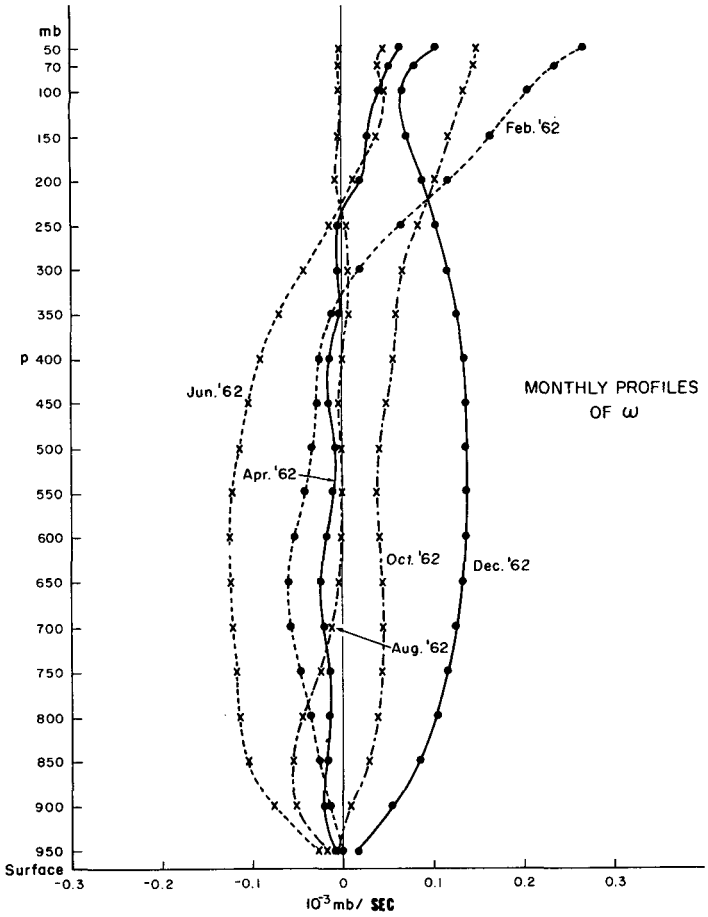

FIGURE 7.—Monthly vertical profiles of the area mean vertical p-velocity.

some energy-generating eddies which are not detected in the present observational network. If this is the case, though not verified, we should have even more dissipation in the free atmosphere than is shown by this study.

To inspect the vertical profiles of the kinetic energy balance, we have to observe the winter (fig. 4) and summer (fig. 5) profiles, along with those of the annual means (fig. 6). Because of the intensified circulation pattern, all energy parameters are large in magnitude during the winter; also, as a result of the upward extension of the maximum wind level, the uppermost part of the balance profile is missing. Because of the large magnitude of the winter energy parameters in the upper part of the atmosphere, the annual balance profile is strongly influenced by the winter type for this part of the atmosphere, especially since the employed time series of the aerological data includes January 1963, when an extremely strong circulation pattern persisted over the North American Continent (see figs. 8 through 11, and also see Kung [5]). Moreover, the magnitude of the horizontal outflow should decrease as the domain of the analysis is expanded beyond North America, and will vanish if the entire global area is covered.

There is a general qualitative agreement between the vertical profiles of the kinetic energy balance presented in this study and those obtained in the general circulation numerical experiment by Smagorinsky, Manabe, and Holloway [15].

In this study, to obtain the vertical transport term, the vertical p-velocity $\bar{\omega}$ was computed by integrating equation (9) vertically upward with the assumption of $\bar{\omega}=0$ at the surface level. When computing the $\bar{\omega}$ in this way, we should recognize that the error in estimating the horizontal wind divergence may accumulate in the upper levels in the process of vertical integration (see Kurihara [7]). Vertical profiles of monthly mean $\bar{\omega}$ are presented in figure 7 for 2-month intervals. In figures 4, 5, and 6, the direction of kinetic energy flux $\overline{\omega k}$ is also indicated by the arrow sign. Though we should be aware of the possibility of accumulated errors in the $\bar{\omega}$ values in the upper part of the atmosphere, we may expect that their effect in this study should be insignificant for two reasons. First, $\partial\bar{\omega}\bar{k}/\partial p$, rather than, $\bar{\omega}\bar{k}$, is used in the study of the energy balance, and probably the error accumulated in $\partial\bar{\omega}\bar{k}/\partial p$ may not be as large as in $\bar{\omega}\bar{k}$. Second, the vertical transport term $\partial\overline{\omega k}/\partial p$ is itself a rather small term in the balance of kinetic energy (see Jensen [3], Holopainen [2], and Smagorinsky, Manabe, and Holloway [15]).

4. BUDGET OF TOTAL KINETIC ENERGY

The vertically integrated mean kinetic energy budgets are presented in table 7 for the four seasons and for the year. Since a discussion of the total kinetic energy budget was given in the previous paper (see Kung [5]), though with a smaller data sample, a general discussion of this matter is not included here.

Regarding the difference between the generation and horizontal outflow as the annual mean "net generation" of the kinetic energy for the domain of analysis, 7.02 watts/m². out of the total generation 9.51 watts/m². approximately balances the annual mean total dissipation of 7.12 watts/m.² A similar balance is also observed throughout four seasons. The annual mean net generation and total dissipation obtained in this study are of the same order of magnitude of, but significantly larger than, the kinetic energy conversion rate 0.91–3.37 watts/m². as compiled by Oort [9] from various sources of observational studies (also see Krueger, Winston, and Haines [4], Saltzman [11], Saltzman and Fleisher [12, 13], Teweles [16], and Wiin-Nielsen, Brown, and Drake [17]). The annual mean total dissipation 7.12 watts/m². is also considerably larger than the currently accepted annual net generation of available potential energy (for example, 2.3 watts/m². as summarized by Oort [9]), which ideally should be equal to the long-term average of the kinetic energy dissipation.

Three reasons may be considered for this obvious discrepancy. First, confinement of the study within the

TABLE 7.—*Vertically integrated seasonal and annual mean kinetic energy budget.* $\overline{k}$ *is in units of* 10^5 *joules/m².* *Other quantities are in watts/m².*

Season	$\overline{k}$	$\frac{\partial \overline{k}}{\partial t}$	$\frac{1}{A}\oint_c \overline{\mathbf{V}k}\cdot n ds$	$\frac{\partial \overline{\omega k}}{\partial p}$	$-\overline{\mathbf{V}\cdot\nabla\phi}$	$-\frac{1}{A}\oint_c \overline{\mathbf{V}k}\cdot n ds$	$\overline{E}$
Winter	26.364	0.758	7.583	−1.219	15.405	7.822	8.283
Spring	16.257	−.234	1.328	.099	8.010	6.682	6.817
Summer	9.075	−.042	.591	.000	7.084	6.493	6.535
Fall	15.474	.258	.464	−.054	7.531	7.067	6.863
Annual mean	16.792	.185	2.492	−.293	9.508	7.016	7.124

TABLE 8.—*Intensity of the annual mean energy process in different portions of the atmosphere.* *Energy level is in units of* 10^5 *joules/m².; generation and dissipation in watts/m².; depletion time in days.* *The percentage shows the distribution of the total in each layer of the atmosphere*

Atmospheric portion	Pressure level (mb.)	Energy level $\overline{k}$	%	Generation $-\overline{\mathbf{V}\cdot\nabla\phi}$	%	Dissipation $\overline{E}$	%	Depletion time $\overline{k}/\overline{E}$
Boundary layer	*969–875	0.338	2	2.209	23	2.211	31	0.18
Layer I	*969–700	1.361	8	4.002	42	4.013	56	0.39
Layer II	700–450	3.459	21	0.642	7	0.418	6	9.58
Layer III	450–200	8.609	51	2.679	28	1.389	20	7.17
Layer IV	200–50	3.363	20	2.185	23	1.304	18	2.98
Total	969–50	16.792	100	9.508	100	7.124	100	2.73

*Area mean surface pressure.

North American Continent may add some regional characteristics to the results obtained. Second, the technique of computational analysis may tend to overestimate. Third, but not the least important, the majority of the currently available observational studies of the energy conversions are largely dependent on the vertical motion calculated with the adiabatic, quasi-geostrophic models from the operationally modified and smoothed geopotential field. The possible underestimate of the energy conversion by this method was discussed by Palmén [10], and Dutton and Johnson [1]. It would be extremely difficult to state which of the above three reasons accounts mainly for the discrepancy at this stage of study. Nevertheless, it presents a very interesting point for investigation in the future.

Dutton and Johnson [1] urge that any calculation of generation of available potential energy which utilizes the approximate formula will be an underestimate. With their exact theory, they give 5.6 watts/m². as the diabatic generation of zonal available potential energy and 0.8 watts/m². as the eddy generation, the sum of which should be equal to the long-term mean of the kinetic energy dissipation.

The annual means of total net generation 7.02 watts/m². and total dissipation 7.12 watts/m². are somewhat higher than the 6.61 watts/m². and 6.38 watts/m². presented in the previous paper (see Kung [5]). This is mainly attributed to inclusion, in the annual average, of the data during the latter two-thirds of January 1963, when the extremely strong circulation pattern prevailed over the North American Continent. The same argument also applies when the total kinetic energy level, horizontal outflow, and generation in this and previous papers are compared.

The total generation in winter 15.41 watts/m². is significantly higher than the 7.08 watts/m². in summer. However, horizontal outflow accounts for about half of the generated kinetic energy, leaving 7.82 watts/m². as the "net generation" in contrast to summer net generation of 6.49 watts/m². Regional characteristics should be studied in further detail in this respect.

Ideally, the vertically integrated vertical transport term $\partial\overline{\omega k}/\partial p$ should vanish when integrated from the surface to the top of the atmosphere. After integration from the surface to the 50-mb. level, $\partial\overline{\omega k}/\partial p$ vanishes for the summer mean, and becomes negligibly small for both spring and fall. For winter, when some significant generation takes place above the 50-mb. level, the total vertical transport amounts to −1.22 watts/m². This represents the kinetic energy supplied to the atmosphere below the 50-mb. level from the higher layers (see also the direction of energy flux $\overline{\omega k}$ in fig. 4). However, the breakdown of the winter total $\partial\overline{\omega k}/\partial p$ is −0.60, 0.01, and −3.06 watts/m². respectively for February and December 1962, and January 1963. The generation above the 50-mb. level is unusually strong during the month of January 1963 (see section 6 and fig. 8), and it is not inconsistent that this month had the largest convergence of $\overline{\omega k}$ below the 50-mb. level.

Incidentally, the vanishing of the vertically integrated vertical transport term may also justify the substitution of $\overline{\omega}\,\overline{k}$ for $\overline{\omega k}$ (see section 2).

5. INTENSITY OF ENERGY PROCESS IN DIFFERENT PORTIONS OF THE ATMOSPHERE

Table 8 shows the kinetic energy level, generation, and dissipation in different layers of the atmosphere in actual physical units, and in percentage of the vertical total, as summarized from tables 2 through 6. The top of the planetary boundary layer is tentatively assumed to be at 875 mb. The atmosphere from the surface to the 50-mb. level is divided into four layers; Layer I from the surface to 700 mb., layer II from 700 mb. to 450 mb., layer III from 450 mb. to 200 mb., and layer IV from 200 mb. to 50 mb. While the amount of kinetic energy contained in the boundary layer and in layers I through IV is respectively 2, 8, 21, 51, and 20 percent of the total $\overline{k}$ on the annual basis, the percentage distribution of the total generation in these layers is 23, 42, 7, 28, and 23 percent, respectively, and the percentage distribution of the total dissipation is 31, 56, 6, 20, and 18 percent. In view of the kinetic energy level in these layers, the energy process is most intense in the lower troposphere, especially in the boundary layer, and least intense in the mid-troposphere where the quasi-geostrophic assumption is usually valid.

In the upper part of the atmosphere, i.e., in layers III and IV, significant portions of the generation and dissipation take place, but about ⅔ of the total kinetic energy is contained in this portion of the atmosphere.

An estimate of the efficiency of the dissipation process in relation to the energy level is the depletion time, which is defined here as $\overline{k}/\overline{E}$, i.e., the time needed to deplete the kinetic energy with a constant dissipation rate when there is no supply of kinetic energy. As shown in table 8, the depletion time is 0.18, 0.39, 9.58, 7.17, and 2.98 days for the boundary layer and layers I, II, III, and IV separately, and 2.73 days for the total kinetic energy. This means that the dissipation process operates much more quickly to deplete the kinetic energy in the lower troposphere, particularly in the boundary layer, than in other portions of the atmosphere. The dissipation is least efficient where the depletion time is very long, i.e., in the mid-troposphere.

The boundary layer dissipation, 2.21 watts/m^2., compares with the previously estimated 1.86 watts/m^2. (see Kung [5]) from Lettau's [8] boundary layer model. It should be noted, however, that the boundary layer dissipation in this study is estimated as a residual from the kinetic energy equation with a tentative top of the boundary layer at the 875-mb. level. With 31 percent of the total dissipation in the boundary layer, the free atmosphere dissipation amounts to 69 percent, or 4.91 watts/m^2. of the total dissipation of 7.12 watts/m^2.

We observe, in table 8 and tables 2 through 6, that the generation and dissipation values are very close in the boundary layer on the annual and seasonal basis. This is not only a feature of the long-time mean, but is also observed throughout the computation on a daily basis. Since the horizontal outflow and vertical transport are both essentially negligible in the kinetic energy budget of this layer for the large-scale domain of analysis, we may recognize an approximate balance of the boundary layer generation and dissipation of kinetic energy in the large-scale atmospheric circulation. This was expected from the previous study (see Kung [5]) using the independently computed generation and dissipation.

The argument concerning the balance of the boundary layer generation and dissipation would not be changed by choosing the top of the boundary layer at 875 mb., since it is a prevalent feature throughout the lower troposphere.

6. SEASONAL CHANGE

Besides the seasonal variations of energy parameters and their balance as presented and discussed elsewhere in this paper, it is interesting to study the seasonal march of the atmospheric energetics. With a time series covering a one-year period, merely a first order conjecture is possible. Nevertheless, it will be interesting to depict the progress of the seasons during this one-year period in terms of time cross sections.

The monthly means of kinetic energy generation, horizontal outflow, and dissipation are plotted separately in figures 8, 9, and 10, as pressure-time cross sections. Figure 11 shows the pressure-time cross section of the mean zonal wind component to express the strength of the circulation pattern during the corresponding period. In figure 8, two major types of generation may be observed, namely winter and summer. The generation in summer is generally weaker than in winter; the level of maximum generation in the upper troposphere rapidly diminishes into the stratosphere in summer; the monthly fluctuation also seems to be small during the summer months. Generally strong generation, significant upward extension of large generation in the upper portion of the atmosphere, and rather large monthly fluctuations characterize the winter part of the cross section. The upward extension of the large generation in winter is apparently related to that of the jet stream level. This is especially evident for January 1963 when the circulation pattern was extremely strong. Transition between winter and summer types of generation is marked by rather abrupt changes of the generation profile in late spring and late fall, namely in May 1962 and November 1962. In those months of abrupt change, the generation in the upper part of the atmosphere suddenly drops to a minimum; the negative generation appears significantly in the stratosphere in May 1962, and the negative generation occupies the mid and upper troposphere in November 1962. This abrupt nature of the seasonal change will be an interesting feature to investigate if it is confirmed by a larger data sample of more than one year.

The pressure-time cross section of figure 9 shows that horizontal outflow of kinetic energy from the continental area roughly resembles the zonal circulation pattern of figure 11 in winter when the zonal wind is very strong. The pressure-time cross section of the dissipation in figure 10 roughly follows the balance of generation and horizontal outflow in figures 8 and 9.

7. EFFECT OF DIURNAL VARIATION ON ESTIMATING ENERGY PARAMETERS

We may expect considerable diurnal variation of the large-scale pattern of wind velocity, and it is of interest to examine the possible effect of data from different times of the day on the estimated energy parameters. While a detailed computation and discussion of this matter are planned for the next phase of this study, 12 GMT aerological data over North America during August and December 1962 were utilized as an example from the same MIT General Circulation Data Library (see section 2) to compute the same energy parameters presented in this study. Examination of the computation with 12 GMT data shows that there is a systematic diurnal variation between the results from 00 and 12 GMT data on the daily basis, which will be an interesting point of investigation. However, the discussion made concerning the balance of the kinetic energy with the 00 GMT data holds for the results with the 12 GMT data as well. Table 9 shows the comparison of the vertically integrated energy parameters with the 00 and 12 GMT data for August and December 1962.

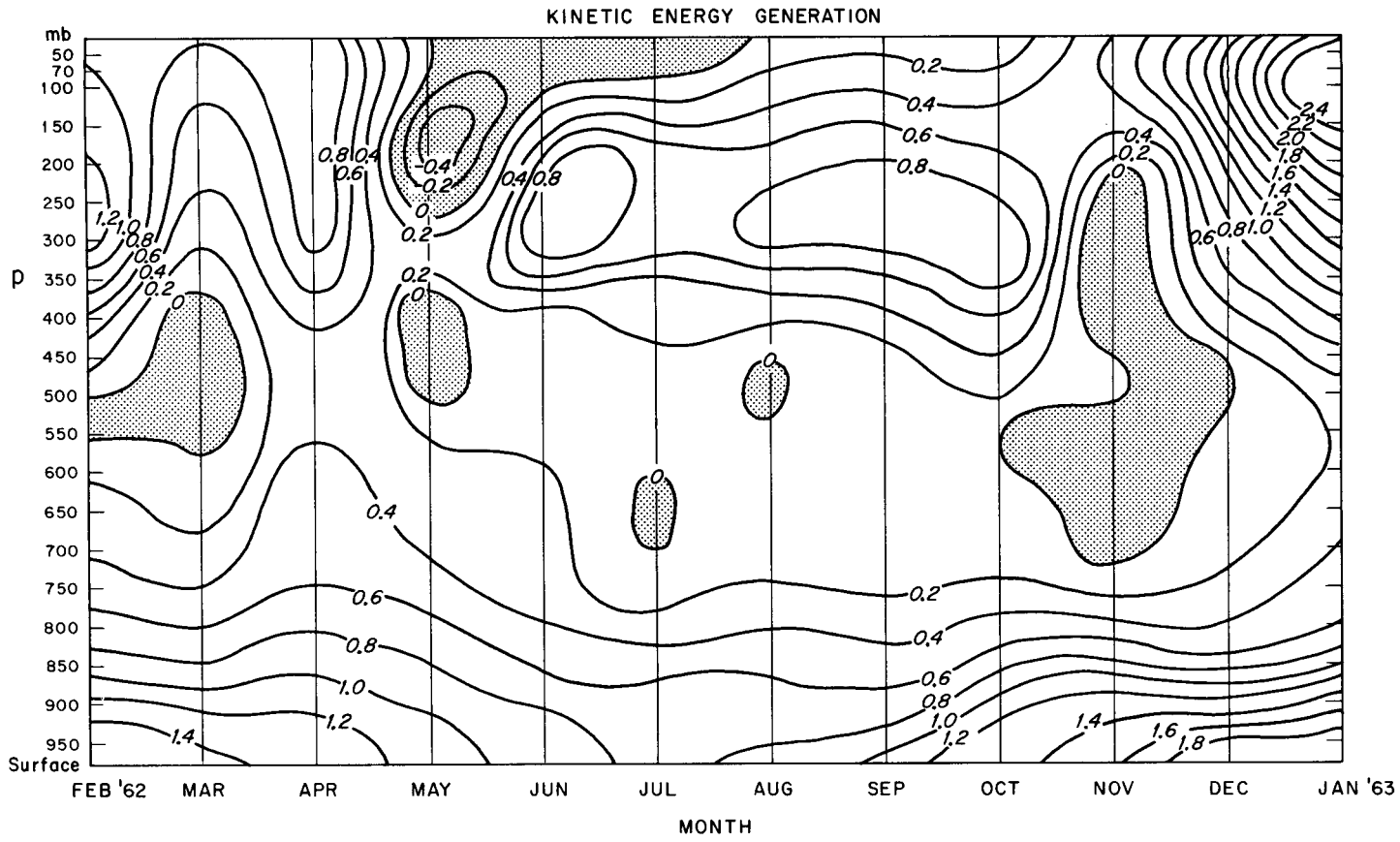

FIGURE 8.—Pressure-time cross section of monthly kinetic energy generation $-\overline{\mathbf{V}\cdot\nabla\phi}$ in units of (watts/m.²)/50 mb. from February 1962 through January 1963. Destruction of kinetic energy is stippled.

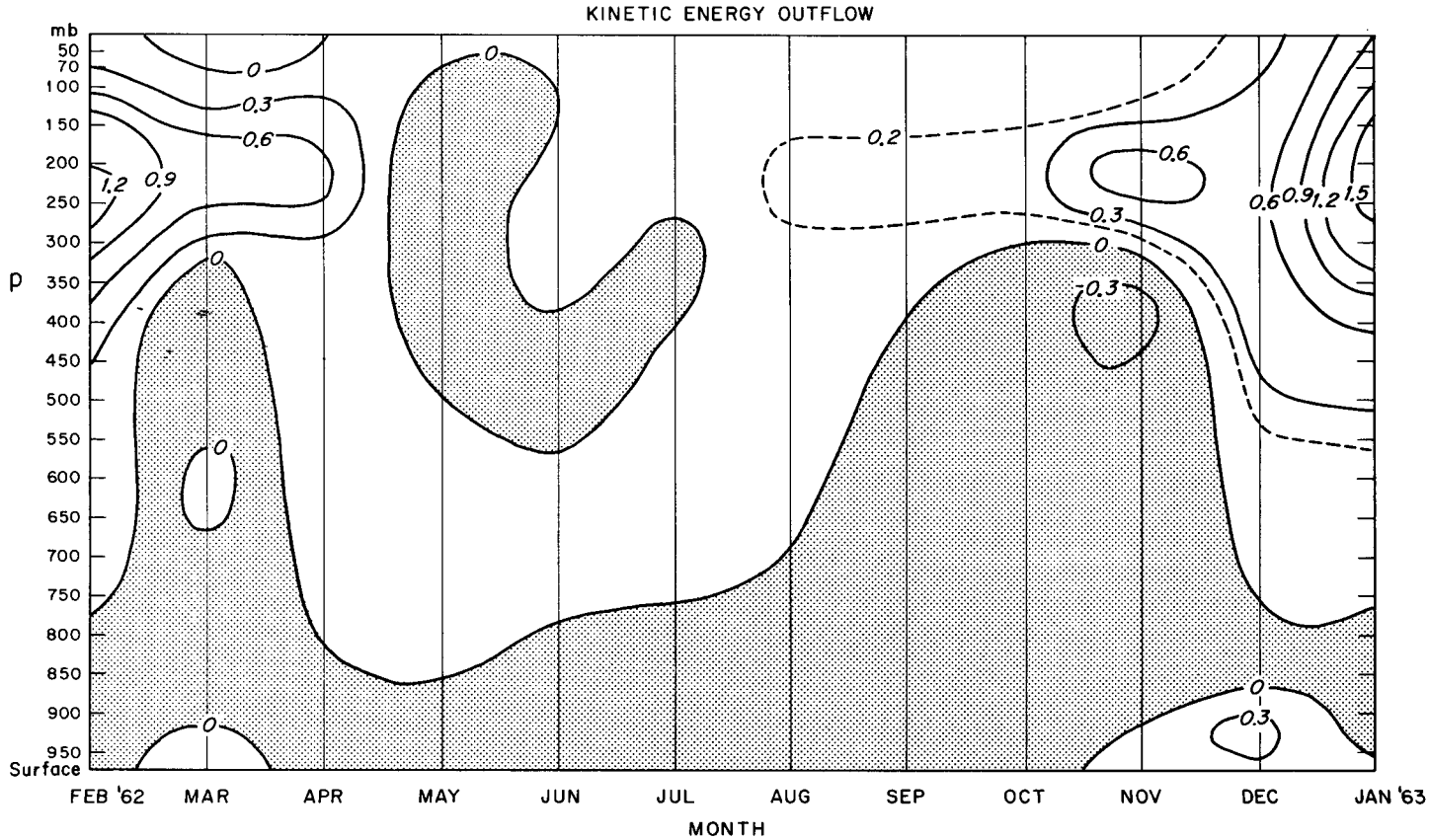

FIGURE 9.—Pressure-time cross section of monthly horizontal outflow of kinetic energy $\frac{1}{A}\oint_c \mathbf{V}k\cdot\mathbf{n}ds$ in units of (watts/m.²)/50 mb. from February 1962 through January 1963. Inflow is stippled.

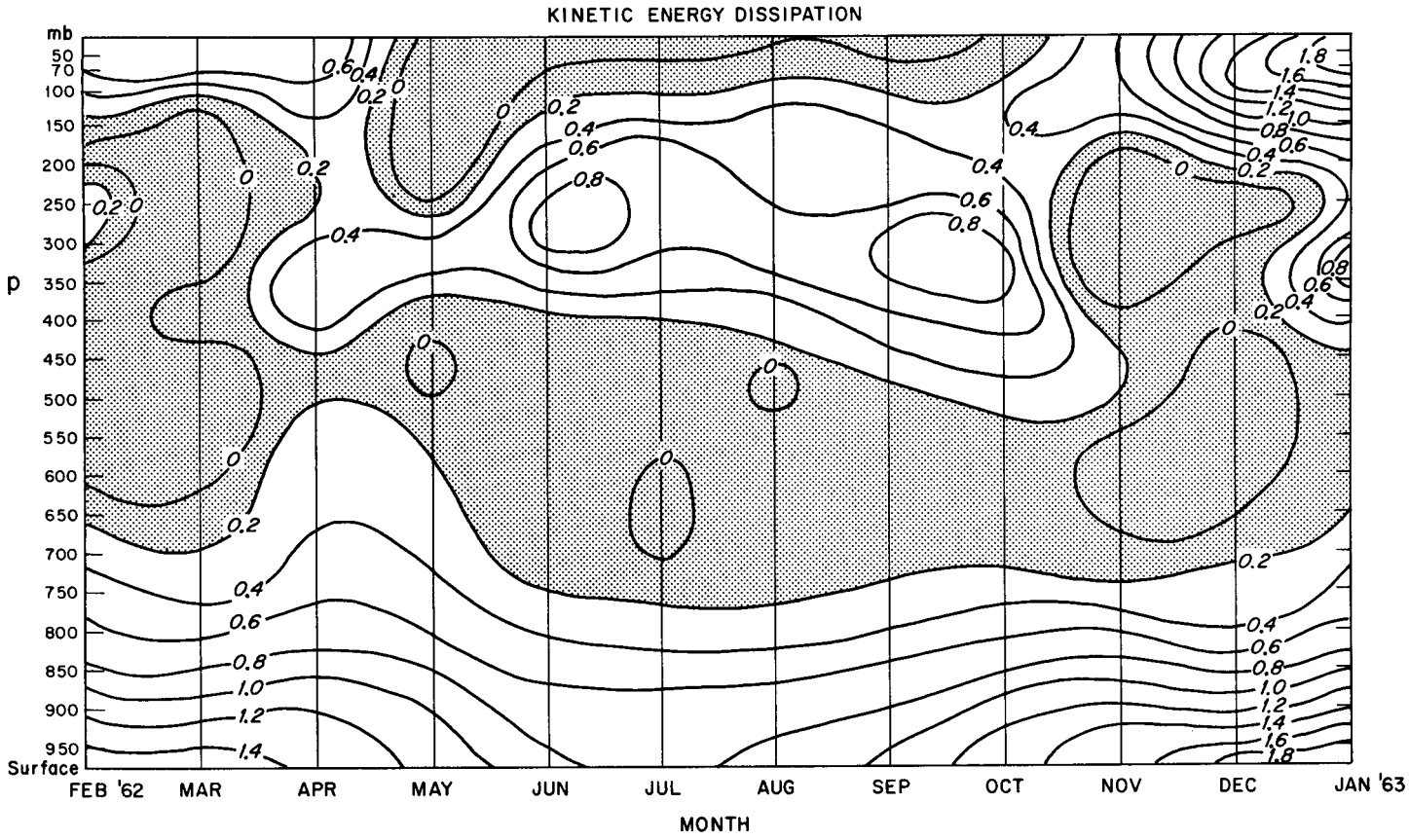

FIGURE 10.—Pressure-time cross section of monthly kinetic energy dissipation $\overline{E}$ in units of (watts/m.²)/50 mb. from February 1962 through January 1963. Dissipation of less than 0.2 (watts/m.²)/50 mb. is stippled.

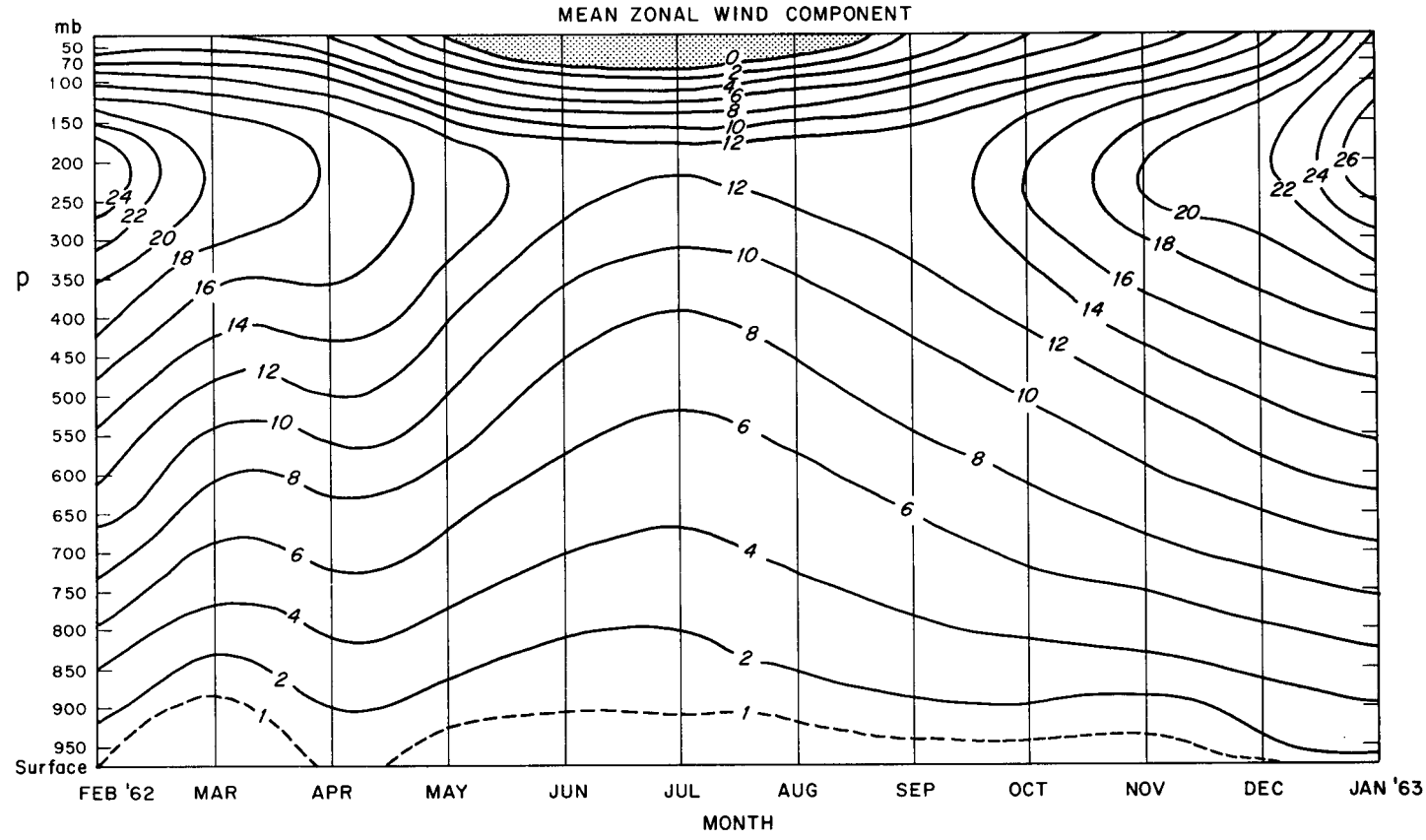

FIGURE 11.—Pressure-time cross section of continental mean of the zonal wind component $\overline{u}$ in units of m./sec. from February 1962 through January 1963.

TABLE 9.—*Comparison of vertically integrated energy parameters with 00 and 12 GMT data for two months. All values are in units of watts/m².*

Month	Time (GMT)	$\frac{\partial \overline{k}}{\partial t}$	$\frac{1}{A}\oint_c \mathbf{V}k\cdot\mathbf{n}ds$	$\frac{\partial \overline{\omega k}}{\partial p}$	$-\overline{\mathbf{V}\cdot\nabla\phi}$	$-\frac{1}{A}\oint_c \mathbf{V}k\cdot\mathbf{n}ds \,/\, -\overline{\mathbf{V}\cdot\nabla\phi}$	$\overline{E}$
August 1962	0000	−0.041	0.979	−0.007	7.316	6.337	6.385
	1200	−.062	−.365	.086	4.588	4.953	4.929
December 1962	0000	.801	4.368	.013	12.099	7.731	6.917
	1200	−.898	2.822	.062	9.211	6.389	7.225

8. SUMMARY

As a further step in a systematic study of the problem of kinetic energy dissipation, attention is focused on the vertical structure and seasonal variation of the kinetic energy balance of the atmosphere. From 11 months' daily wind and geopotential data during 1962 and 1963 over North America, the generation $-\overline{\mathbf{V}\cdot\nabla\phi}$, local change $\partial\overline{k}/\partial t$, horizontal outflow $1/A\oint \mathbf{V}k\cdot\mathbf{n}ds$, and vertical transport $\partial\overline{\omega k}/\partial p$ are evaluated for 20 pressure layers from the surface to the 50-mb. level. The dissipation is then obtained as the residual required to balance the kinetic energy equation.

The direct evaluation of the generation $-\overline{\mathbf{V}\cdot\nabla\phi}$ is essential for studying not only the vertical structure of the kinetic energy balance but also the problem of energy conversion itself. The generation is the most dominant term among the directly computed parameters of the energy process; the horizontal outflow is the next most important; the vertical transport is rather insignificant except in winter; and the local change is the least significant.

Observing the vertical profiles of the kinetic energy balance, we find a maximum of generation in the planetary boundary layer; it gradually decreases toward a minimum in the mid-troposphere, increases again toward the second maximum in the upper part of the atmosphere, and then decreases again into the stratosphere. The vertical profile of the dissipation generally follows that of the generation. In the lower troposphere, particularly in the boundary layer, the generation and dissipation values are nearly equal, while other parameters are negligibly small. In the mid-troposphere, all parameters of the energy process have small numerical values. In the upper part of the atmosphere, the dissipation is also at a maximum in accordance with the generation, but the horizontal outflow and vertical transport contribute significantly to the kinetic energy balance.

The annual means of the vertically integrated total generation, net generation (i.e., the difference of total generation and horizontal outflow), and dissipation are 9.51, 7.02, and 7.12 watts/m²., respectively. These values are significantly higher than the currently accepted conversion rate from available potential energy. Regional confinement of the study to a continental area or some systematic overestimate in this study may be considered responsible for this discrepancy. However, we cannot exclude the possibility that the currently accepted values, obtained by calculating the vertical motion from the adiabatic, quasi-geostrophic model using operationally modified and smoothed geopotential data, are too low.

By tentatively taking the 875-mb. level as the top of the planetary boundary layer, 2.21 watts/m². or 31 percent of the total dissipation of 7.12 watts/m². is regarded as the boundary layer dissipation, and 4.91 watts/m². or 69 percent of the total dissipation may in turn be regarded as the free atmosphere dissipation. For the large-scale domain of analysis we may recognize an approximate balance between the kinetic energy generation and dissipation in the boundary layer. This is also a prevalent feature throughout the lower troposphere.

In view of the amount of kinetic energy contained in different portions of the atmosphere, the energy processes of kinetic energy generation and dissipation are most intense in the lower troposphere, particularly in the boundary layer, and least intense in the mid-troposphere. Significant portions of the generation and dissipation take place in the upper part of the atmosphere, but about ⅔ of the total kinetic energy is involved there.

In terms of depletion time, the dissipation process operates most efficiently in the lower troposphere in general and in the boundary layer in particular, and it operates most inefficiently in the mid-troposphere. The depletion times for the boundary layer, lower troposphere, and the mid-troposphere are 0.18, 0.39, and 9.58 days respectively; it is 7.17 days for the layer between 450 mb. and 200 mb., and 2.98 days for the layer between 200 mb. and 50 mb.

In plots of the pressure-time cross sections of monthly energy parameters, a seasonal change of the atmospheric energetics is depicted for the one-year period. Winter type and summer type patterns are recognized, while a rather abrupt transition between these two types takes place in late spring and late fall.

9. REMARK

A comment should be made about the quality of data used in this study. As exemplified in table 1, the coverage of aerological data has become fairly good in recent years over North America and some other parts of the Northern Hemisphere even to a relatively high altitude. The network is fairly dense even after missing data are eliminated, and the suspicious records are rare. Besides the observational improvements, the data quality owes very much to the efforts in data editing and compiling of the MIT General Circulation Data Library under the direction of Professor V. P. Starr.

The results obtained in this study point to an extension of the study along the following lines:

(1) Extension of the domain of analysis beyond North

America to include other parts of the Northern Hemisphere.

(2) Use of a larger data sample over an extended period.

(3) Study of the dissipation by various mechanisms and its incorporation into the numerical models of the large-scale atmospheric circulation.

ACKNOWLEDGMENTS

The courtesy of Professor V. P. Starr of the Massachusetts Institute of Technology and the kind assistance of Mr. H. M. Frazier of the Travelers Research Center, Inc. and Mr. S. F. Seroussi of the Mitre Corporation in arranging the input data are gratefully acknowledged. The author is also greatly indebted to Professor Starr for his most valuable comments and suggestions. The very constructive comments from Professors R. A. Bryson and D.R. Johnson of the University of Wisconsin and Professor J. A. Dutton of the Pennsylvania State University are sincerely appreciated.

The author is very grateful to Dr. S. Manabe and Dr. J. Smagorinsky for their encouraging interest and fruitful discussions, and to Mr. R. D. Graham for providing various necessary arrangements. The author also would especially like to thank Dr. J. Smagorinsky, Dr. S. Manabe, Dr. E. M. Rasmusson, Dr. A. H. Oort, and Mr. S. Hellerman for reviewing the original manuscript. The help of Mr. W. H. Moore and Miss M. Saffell and Mrs. C. Bunce in preparing the manuscript is very much appreciated.

REFERENCES

1. J. A. Dutton and D. R. Johnson, "The Theory of Available Potential Energy and a Variation Approach to Atmospheric Energetics," 1966. (To be published in *Advances in Geophysics.*)
2. E. O. Holopainen, "Investigation of Friction and Diabatic Processes in the Atmosphere," Paper No. 101, Dept. of Meteorology, University of Helsinki, 1964, 47 pp.
3. C. E. Jensen, "Energy Transformation and Vertical Flux Process over the Northern Hemisphere," *Journal of Geophysical Research*, vol. 66, No. 4, Apr. 1961, pp. 1145–1156.
4. A. F. Krueger, J. S. Winston, and D. A. Haines, "Computation of Atmospheric Energy and its Transformation for the Northern Hemisphere for a Recent Five-Year Period," *Monthly Weather Review*, vol. 93, No. 4, Apr. 1965, pp. 227–238.
5. E. C. Kung, "Kinetic Energy Generation and Dissipation in the Large-Scale Atmospheric Circulation," *Monthly Weather Review*, vol. 94, No. 2, Feb. 1966, pp. 67–82.
6. E. C. Kung, R. A. Bryson, and D. H. Lenschow, "Study of a Continental Surface Albedo on the Basis of Flight Measurements and Structure of the Earth's Surface Cover over North America," *Monthly Weather Review*, vol. 92, No. 12, Dec. 1964, pp. 543–564.
7. Y. Kurihara, "Accuracy of Wind-aloft Data and Estimation of Error in Numerical Analysis of Atmospheric Motions," *Journal of Meteorological Society of Japan*, Series II, vol. 39, No. 6, Dec. 1961, pp. 331–345.
8. H. H. Lettau, "Theoretical Wind Spirals in the Boundary Layer of a Barotropic Atmosphere," *Beiträge zur Physik der Atmosphäre*, vol. 35, No. 314, 1962, pp. 195–212.
9. A. H. Oort, "On Estimates of the Atmospheric Energy Cycle," *Monthly Weather Review*, vol. 92, No. 11, Nov. 1964, pp. 483–493.
10. E. Palmén, "On Generation and Frictional Dissipation of Kinetic Energy in the Atmosphere," *Societas Scientiarum Fennica, Commentationes Physico-Mathematicae*, vol. 24, No. 11, 1960, 15 pp.
11. B. Saltzman, "The Zonal Harmonic Representation of the Atmospheric Energy Cycle—A Review of Measurements," The Travelers Research Center, Report TRC–9, Sept. 1961, 19 pp.
12. B. Saltzman and A. Fleisher, "Spectrum of Kinetic Energy Transfer Due to Large-Scale Horizontal Reynolds Stress," *Tellus*, vol. 12, No. 1, Feb. 1960, pp. 110–111.
13. B. Saltzman and A. Fleisher, "Further Statistics of the Modes of Release of Available Potential Energy," *Journal of Geophysical Research*, vol. 66, No. 7, July 1961, pp. 2271–2273.
14. J. Smagorinsky, "General Circulation Experiment with the Primitive Equations. 1. The Basic Experiment," *Monthly Weather Review*, vol. 91, No. 3, Mar. 1963, pp. 99–164.
15. J. Smagorinsky, S. Manabe, and J. L. Holloway, Jr., "Numerical Results from a Nine-Level General Circulation Model of the Atmosphere," *Monthly Weather Review*, vol. 93, No. 12, Dec. 1965, pp. 727–768.
16. S. Teweles, "Spectral Aspects of the Stratospheric Circulation during the IGY," Report No. 8, Dept. of Meteorology, Massachusetts Institute of Technology, Jan. 1963, 191 pp.
17. A. Wiin-Nielsen, J. A. Brown, and M. Drake, "On Atmospheric Energy Conversion between the Zonal Flow and the Eddies," *Tellus*, vol. 15, No. 3, Aug. 1963, pp. 261–279.

[*Received August 31, 1966; revised September 27, 1966*]